

Continuous solid solutions $\text{LiFe}_{1-x}\text{Co}_x\text{PO}_4$ and its electrochemical performance

Deyu Wang, Zhaoxiang Wang, Xuejie Huang, Liquan Chen*

Laboratory for Solid State Ionics, Institute of Physics, Chinese Academy of Sciences, Beijing 100080, China

Available online 27 April 2005

Abstract

$\text{LiFe}_{1-x}\text{Co}_x\text{PO}_4$ ($0 \leq x \leq 1.0$) solid solutions were prepared by solid-state reactions. X-ray diffraction and X-ray photoelectron spectroscopy were employed to analyze the variation of their structures and the chemical environments around the P and O atoms of the solid solution with various Co contents. The electrochemical performance of $\text{LiFe}_{1-x}\text{Co}_x\text{PO}_4$ was also comparatively studied with cyclic voltammetry, and galvanostatic charge–discharge.

© 2005 Elsevier B.V. All rights reserved.

Keywords: Solid solution; $\text{LiFe}_{1-x}\text{Co}_x\text{PO}_4$

1. Introduction

In recent years, considerable attention has been paid to develop cathode materials for lithium ion batteries with high capacity, safety, and reliability. Since the pioneering work of Goodenough and coworkers [1] on LiFePO_4 , much effort has been made to improve the performance of this material [2–12]. Other LiMPO_4 ($M = \text{Co}, \text{Mn}, \text{and Ni}$) olivine-structured materials have also been investigated as attractive cathode candidates due to their higher theoretical capacity and/or energy density than that of LiFePO_4 [13–16]. Among these materials, LiCoPO_4 is expected to have a high energy density due to its 4.8 V discharge plateau.

In addition to the olivines with single transition metal atoms, olivine solid solutions are become attractive recently. For example, the charge–discharge profiles of $\text{LiFe}_{1-x}\text{Mn}_x\text{PO}_4$ [17–21] show two pairs of voltage plateaus, one at 4.1 V and the other at 3.5 V, corresponding to the conversions of $\text{Mn}^{2+} \leftrightarrow \text{Mn}^{3+}$ and $\text{Fe}^{2+} \leftrightarrow \text{Fe}^{3+}$, respectively. However, some of these solid solutions have obvious amount of Li_3PO_4 impurity [22].

In this paper, we will report the preparation of a series of pure $\text{LiFe}_{1-x}\text{Co}_x\text{PO}_4$ solid solutions and evaluate their elec-

trochemical performances as cathode materials for lithium ion batteries.

2. Experimental

$\text{LiFe}_{1-x}\text{Co}_x\text{PO}_4$ ($0 \leq x \leq 1.0$) was prepared by solid state reactions. Stoichiometric amounts of $\text{FeC}_2\text{O}_4 \cdot 2\text{H}_2\text{O}$ (99%, Aldrich), $\text{Co}(\text{AC})_2 \cdot 4\text{H}_2\text{O}$ (99%, Beijing Chemicals), $\text{NH}_4\text{H}_2\text{PO}_4$ (99.5%, Beijing Chemicals) and LiF [23] (99.99%, Beijing Chemicals) were mixed and ball-milled for 3 h. The mixture was sintered in a tube furnace with flowing Ar-H_2 mixture (92:8, v/v) at 400°C for 8 h. After cooled down to room temperature, the samples were re-ground and kept at 600°C for 24 h in the same atmosphere.

$\text{LiFe}_{1-x}\text{Co}_x\text{PO}_4$ electrode was prepared with $\text{LiFe}_{1-x}\text{Co}_x\text{PO}_4$, carbon black and polyvinylidene fluoride (PVDF) at a weight ratio of 75:15:10 with Al foil as the current collector. Lithium foil was used as the counter electrode, 1 mol L^{-1} LiPF_6 dissolved in ethylene carbonate/dimethyl carbonate (1:1, v/v) as electrolyte, and Celgard® 2300 as the separator. Test cells were assembled in an MBraun glove box filled with pure argon. The cell was cycled between 2.0 and 4.95 V on a Land battery tester (Wuhan, China) at room temperature. The cell was first charged to 4.95 V at a constant current density and then kept at that voltage until the current density faded to less

* Corresponding author.

E-mail addresses: wangzx@aphy.iphy.ac.cn (Z. Wang), lqchen@aphy.iphy.ac.cn (L. Chen).

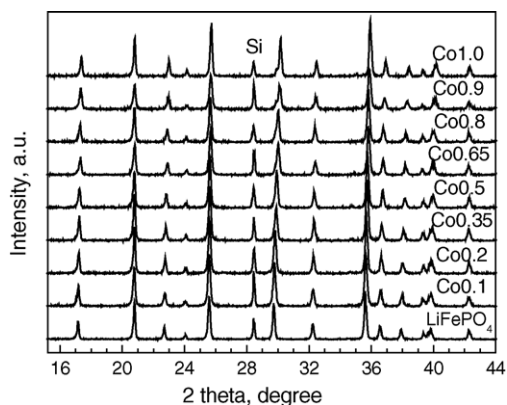


Fig. 1. The XRD pattern of $\text{LiFe}_{1-x}\text{Co}_x\text{PO}_4$.

than 0.1 mA g^{-1} . Cyclic voltammetry (CV) was carried out between 2.7 and 5.2 V at a scan rate of 0.05 mV s^{-1} on CHI660A electrochemical workstation at room temperature.

D/MAX-RC X-ray diffractometer (XRD) with Cu $K\alpha$ radiation was used to characterize the structure and phase purity of these materials. X-ray photoelectron spectroscopy (XPS) analysis was carried out on Sigma Probe (Thermo VG Scientific Co. Ltd.) to probe the chemical environments around the O and P atoms in the material.

3. Results and discussion

Fig. 1 shows the XRD patterns of $\text{LiFe}_{1-x}\text{Co}_x\text{PO}_4$ solid solutions. All samples show well-defined olivine structures. No diffraction peaks belonging to Li_3PO_4 are recognized in the XRD patterns of the LiFePO_4 , LiCoPO_4 and their solid solutions. Both LiFePO_4 and LiCoPO_4 show ordered olivine structures belonging to orthorhombic $pnmb$. Calculation indicates that the difference of lattice constants between LiFePO_4 and LiCoPO_4 is very small, $a = 10.32 \text{ \AA}$, $b = 6.01 \text{ \AA}$, $c = 4.69 \text{ \AA}$ and $V = 290.9 \text{ \AA}^3$ for LiFePO_4 versus $a = 10.20 \text{ \AA}$, $b = 5.92 \text{ \AA}$, $c = 4.70 \text{ \AA}$ and $V = 283.8 \text{ \AA}^3$ for LiCoPO_4 .

Fig. 2 shows the dependence of the orthorhombic lattice parameters on the Co content. The a and b values of the

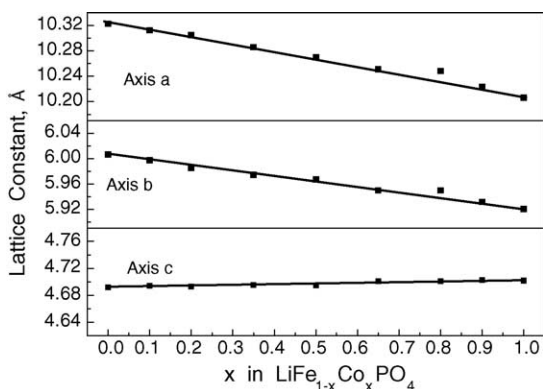
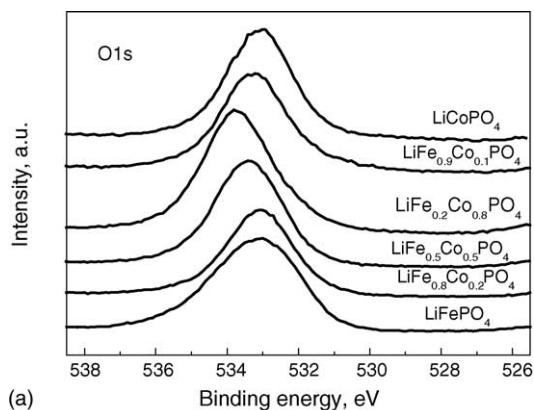
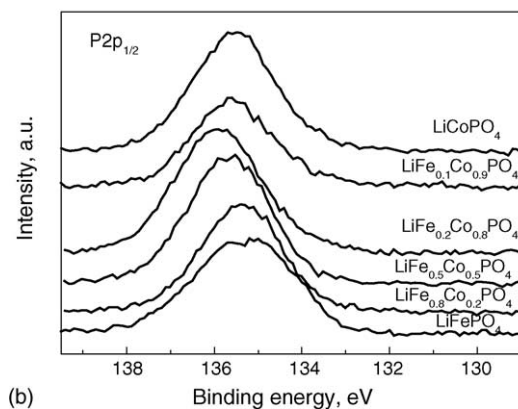


Fig. 2. Variation of the lattice constants as a function of x in $\text{LiFe}_{1-x}\text{Co}_x\text{PO}_4$.



(a)



(b)

Fig. 3. The XPS spectra of O 1s (a) and P $2p_{1/2}$ (b).

prepared samples vary linearly with the increasing Co content except for that of the $\text{LiFe}_{0.2}\text{Co}_{0.8}\text{PO}_4$ which deviates from the linear relationship.

The variation of the chemical environments of O and P in the solid solutions with different Co contents is studied by XPS (Fig. 3). The O 1s peak of LiFePO_4 is at 533.2 and is enhanced with increasing Co content in the solid solution (Fig. 3a). It reaches 533.7 eV in $\text{LiFe}_{0.2}\text{Co}_{0.8}\text{PO}_4$ but then decreases when the Co content is further increased. The O 1s peak is at 533.1 eV for LiCoPO_4 . The changing rule of P $2p_{1/2}$ binding energy (Fig. 3b) is the same as that of O 1s.

Clearly, $\text{LiFe}_{0.2}\text{Co}_{0.8}\text{PO}_4$ shows the highest O 1s binding energy in all the samples. Considering that the dependence of its cell parameters deviates obviously from the linear relationship of a or b versus the Co content, it seems that $x = 0.2$ is a critical point for the properties of the material. The obvious deviation of $\text{LiFe}_{0.2}\text{Co}_{0.8}\text{PO}_4$ is tentatively attributed to the change of M–O (M = Fe, Co) interaction at different Co contents.

The CV curves of LiFePO_4 , $\text{LiFe}_{0.5}\text{Co}_{0.5}\text{PO}_4$ and LiCoPO_4 are compared in Fig. 4. As the electrolyte will be severely decomposed above 5.0 V, the charge cut-off voltage is set at 4.95 V for the CV and 4.90 V for the charge–discharge cycling. As shown in Fig. 4, the oxidation–reduction peaks of LiFePO_4 and LiCoPO_4 are centered at around 3.5 and 4.8 V, respectively. Two pairs of peaks are found in the CV of

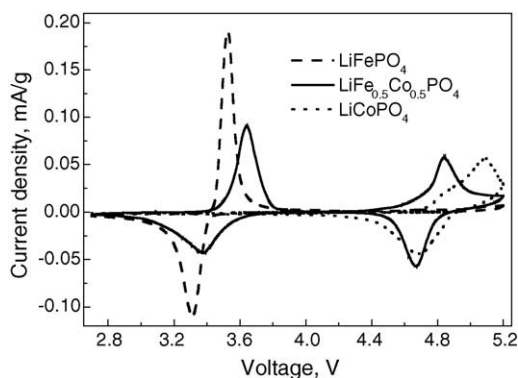


Fig. 4. The CV curves of $\text{LiFe}_{1-x}\text{Co}_x\text{PO}_4$, $x=0, 0.2, 0.5, 0.8, 1.0$. The cells were cycled between 2.7 and 5.2 V at a scan rate of 0.05 mV s^{-1} .

$\text{LiFe}_{0.5}\text{Co}_{0.5}\text{PO}_4$. Similar to $\text{LiFe}_{1-x}\text{Mn}_x\text{PO}_4$, the peaks near 4.8 V are the reaction of $\text{Co}^{2+}/\text{Co}^{3+}$, and the peaks around 3.4 V correspond the reaction of $\text{Fe}^{2+}/\text{Fe}^{3+}$. This indicates that Co and Fe are oxidized or reduced subsequently during charge and discharge. This also verifies that $\text{LiFe}_{0.5}\text{Co}_{0.5}\text{PO}_4$ (and analogously other $\text{LiFe}_{1-x}\text{Co}_x\text{PO}_4$ materials here) is a solid solution. Meanwhile, the redox potential of the $\text{Fe}^{2+}/\text{Fe}^{3+}$ couple is 100 mV higher than in LiFePO_4 while that for the $\text{Co}^{2+}/\text{Co}^{3+}$ couple is about 100 mV lower than in LiCoPO_4 . In this sense, the solid solution is different from a simple mixture of LiFePO_4 and LiCoPO_4 . The interference between Co and Fe changes the Fermi level or the structure of the energy band of each obviously. This explains the variation of the binding energy of O 1s and P 2p_{1/2} in the above XPS study.

Table 1 lists the reduction and oxidation potentials of the series of materials in CV curves.

The charge profiles of the solid solutions are compared in Fig. 5A. All the cells were charged to 4.90 V at the same current density, 2 mA g^{-1} . LiCoPO_4 shows the lowest charge capacity (135 mAh g^{-1}) with a voltage plateau at 4.90 V for the $\text{Co}^{2+} \rightarrow \text{Co}^{3+}$ conversion. In the solid solutions with $x=0.2, 0.5$ and 0.8 , this plateau shifts to 4.82, 4.78, and 4.75 V respectively, consistent with the above CV results.

The discharge profiles of the solid solutions are shown in Fig. 5B. LiFePO_4 has a capacity of 164 mA g^{-1} , close to its theoretical capacity (170 mA g^{-1}). However, LiCoPO_4 exhibits only a capacity of 85 mA g^{-1} with a discharge plateau around 4.74 V, much lower than its theoretical capac-

Table 1

Comparison of the redox potentials of solid solutions with different Co contents

	$\text{Fe}^{2+} \leftrightarrow \text{Fe}^{3+}$		$\text{Co}^{2+} \leftrightarrow \text{Co}^{3+}$	
	Charge	Discharge	Charge	Discharge
$\text{Co}_{0.0}$	3.526	3.310	–	–
$\text{Co}_{0.2}$	3.612	3.344	4.755	4.642
$\text{Co}_{0.5}$	3.631	3.374	4.840	4.667
$\text{Co}_{0.8}$	3.673	3.378	4.999	4.682
$\text{Co}_{1.0}$	–	–	5.087	4.687

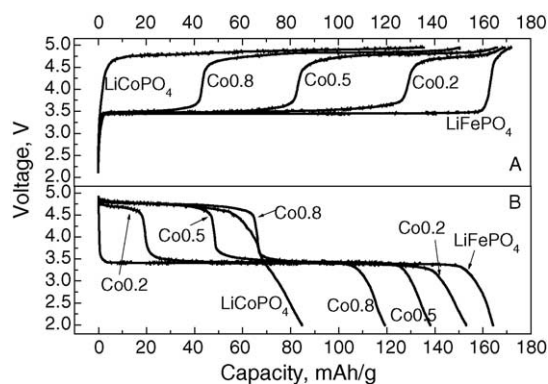


Fig. 5. The charge (A) and discharge (B) plateaus of $\text{LiFe}_{1-x}\text{Co}_x\text{PO}_4$ with $x=0, 0.2, 0.5, 0.8, 1.0$.

ity (165 mA g^{-1}). The capacity of $\text{LiFe}_{1-x}\text{Co}_x\text{PO}_4$ at $x=0.2, 0.5, 0.8$ is 153, 138, and 119 mA g^{-1} , respectively. The contribution of the reaction $\text{Co}^{2+} \leftrightarrow \text{Co}^{3+}$ to the capacity should be around 110 mA g^{-1} for LiCoPO_4 , assuming that the contribution of the $\text{Fe}^{2+} \leftrightarrow \text{Fe}^{3+}$ conversion in solid solution is the same as in LiFePO_4 . This indicates that more capacity from $\text{Co}^{2+} \leftrightarrow \text{Co}^{3+}$ conversion can be utilized or this conversion can be more complete in the solid solutions than in LiCoPO_4 . The reason might be that the potential for the $\text{Co}^{2+} \rightarrow \text{Co}^{3+}$ reaction is lower in the solid solution than in LiCoPO_4 and this reaction finishes below the charge cut-off voltage.

The cyclic performance of $\text{LiFe}_{1-x}\text{Co}_x\text{PO}_4$ is shown in Fig. 6. The cells were cycled at a current density of 10 mA g^{-1} . LiFePO_4 and LiCoPO_4 exhibit poor cyclic performance, only 76.2% and 58.2% the capacity of the first cycle can be remained after 20 cycles for LiFePO_4 and LiCoPO_4 , respectively. On the contrary, the solid solution samples keep a rather high capacity in 20 cycles, remaining 88.4% of the original capacity for $\text{LiFe}_{0.8}\text{Co}_{0.2}\text{PO}_4$, 86.3% for $\text{LiFe}_{0.5}\text{Co}_{0.5}\text{PO}_4$, and 88.1% for $\text{LiFe}_{0.2}\text{Co}_{0.8}\text{PO}_4$. Particle cracking is one of the reasons for the capacity loss of LiFePO_4 [24]. Electrolyte decomposition should be another reason for the capacity fade of the solid solutions as well as for LiCoPO_4 .

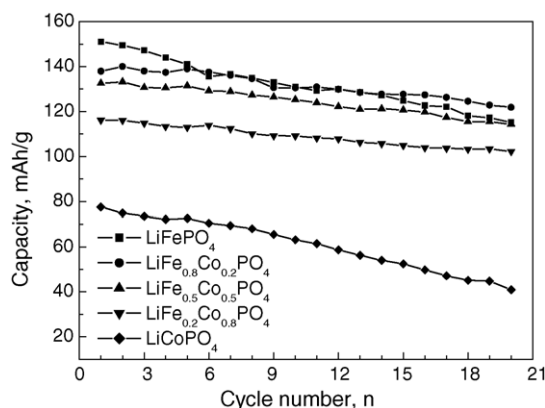


Fig. 6. The cyclic performance of $\text{LiFe}_{1-x}\text{Co}_x\text{PO}_4$.

4. Conclusion

The structure, electrochemical performances and the chemical environments around the O and P atoms of LiFePO_4 , LiCoPO_4 and their solid solutions are compared as cathode materials for lithium ion batteries. The Formation of a solid solution lowers the oxidation potential of the Co^{2+} ions and make the $\text{Co}^{2+} \rightarrow \text{Co}^{3+}$ reaction complete at a lower voltage. As a result, this reaction makes more contribution of capacity in the solid solution than in LiCoPO_4 .

Acknowledgement

This work was supported by the National 973 Program of China (Contract No. 2002CB211802).

References

- [1] A. Padhi, K. Nanjundaswamy, J. Goodenough, J. Electrochem. Soc. 144 (1997) 1188.
- [2] A. Yamada, S. Chung, K. Hinokuma, J. Electrochem. Soc. 148 (2001) A224.
- [3] N. Ravet, J. Goodenough, et al., Proceedings of the 196th Meeting of the Electrochemical Society, vol. 127, Hawaii, USA, 1999.
- [4] H. Huang, S. Yin, L. Nazar, Electrochem. Solid-State Lett. 4 (2001) A170.
- [5] S. Franger, F. Le Cras, et al., Electrochem. Solid-State Lett. 5 (2002) A231.
- [6] G. Li, H. Azuma, M. Tohda, J. Electrochem. Soc. 149 (2002) A743.
- [7] Z. Chen, J.R. Dahn, J. Electrochem. Soc. 149 (2002) A1184.
- [8] N. Ravet, Y. Chouinard, et al., J. Power Sources 97/98 (2001) 503.
- [9] S. Yang, Y. Song, et al., Electrochem. Commun. 4 (2002) 239.
- [10] F. Croce, A. Epifanio, et al., Electrochem. Solid-State Lett. 5 (2002) A47.
- [11] S. Chung, J. Bloking, Y. Chiang, Nat. Mater. 2 (2002) 123.
- [12] S.Q. Shi, L.J. Liu, C.Y. Ouyang, D.S. Wang, Z.X. Wang, L.Q. Chen, X.J. Huang, Phys. Rev. B 68 (2003) 195108.
- [13] K. Amine, H. Yasuda, M. Yamach, Electrochem. Solid-State Lett. 3 (2000) 178.
- [14] S. Okada, S. Sawa, et al., J. Power Sources 97/98 (2001) 430.
- [15] J. Lloris, C. Vicente, J. Tirado, Electrochem. Solid-State Lett. 5 (2002) A234.
- [16] G. Li, H. Azuma, M. Tohda, Electrochem. Solid-State Lett. 5 (2002) A135.
- [17] G. Li, Y. Kudo, et al., J. Electrochem. Soc. 149 (2002) A1414.
- [18] G. Li, H. Azuma, M. Tohda, J. Electrochem. Soc. 149 (2002) A743.
- [19] A. Yamada, Y. Kudo, K. Liu, J. Electrochem. Soc. 148 (2001) A747.
- [20] A. Yamada, S. Chung, J. Electrochem. Soc. 148 (2001) A960.
- [21] A. Yamada, Y. Kudo, K. Liu, J. Electrochem. Soc. 148 (2001) A1153.
- [22] N. Penazzi, M. Arrabito, et al., J. Eur. Ceram. Soc. 24 (2004) 1381.
- [23] D.Y. Wang, L.Q. Chen, et al., J. Solid State Chem. 177 (2004) 4582.
- [24] D. Wang, X. Wu, Z. Wang, L. Chen, J. Power Sources 140 (2005) 125.